



Published in final edited form as:

Atmos Environ (1994). 2013 April ; 68: 198–207. doi:10.1016/j.atmosenv.2012.11.019.

Computational fluid dynamics modeling of transport and deposition of pesticides in an aircraft cabin

Sastry S. Isukapalli^a, Sagnik Mazumdar^a, Pradeep George^a, Binnian Wei^a, Byron Jones^b, and Clifford P. Weisel^{a,*}

^aEnvironmental and Occupational Health Sciences Institute (EOHSI), A Joint Institute of UMDNJ-RW Johnson Medical School & Rutgers University, Piscataway, NJ, USA

^bKansas State University, Manhattan, KS, USA

Abstract

Spraying of pesticides in aircraft cabins is required by some countries as part of a disinsection process to kill insects that pose a public health threat. However, public health concerns remain regarding exposures of cabin crew and passengers to pesticides in aircraft cabins. While large scale field measurements of pesticide residues and air concentrations in aircraft cabins scenarios are expensive and time consuming, Computational Fluid Dynamics (CFD) models provide an effective alternative for characterizing concentration distributions and exposures. This study involved CFD modeling of a twin-aisle 11 row cabin mockup with heated manikins, mimicking a part of a fully occupied Boeing 767 cabin. The model was applied to study the flow and deposition of pesticides under representative scenarios with different spraying patterns (sideways and overhead) and cabin air exchange rates (low and high). Corresponding spraying experiments were conducted in the cabin mockup, and pesticide deposition samples were collected at the manikin's lap and seat top for a limited set of five seats. The CFD model performed well for scenarios corresponding to high air exchange rates, captured the concentration profiles for middle seats under low air exchange rates, and underestimated the concentrations at window seats under low air exchange rates. Additionally, both the CFD and experimental measurements showed no major variation in deposition characteristics between sideways and overhead spraying. The CFD model can estimate concentration fields and deposition profiles at very high resolutions, which can be used for characterizing the overall variability in air concentrations and surface loadings. Additionally, these model results can also provide a realistic range of surface and air concentrations of pesticides in the cabin that can be used to estimate potential exposures of cabin crew and passengers to these pesticides.

Keywords

CFD; Pesticide; Pyrethroid; Permethrin; Airliner cabin; Disinsection

1. Introduction

Aircraft cabin disinsection with pesticide spraying has been in practice since the 1920s (Rayman, 2006). Even though it is no longer routinely practiced in many countries, countries such as China and India require disinsection of all in-bound flights with a pesticide spray while passengers are on board (USDOT, 2010). Countries such as Australia and New Zealand require similar disinsection spraying, but allow, as an alternative, residual pesticide treatment of aircraft (typically once every 6–8 weeks), which is performed in unoccupied cabins (USDOT, 2010). Countries such as France and United Kingdom also require disinsection with pesticide spraying while passengers are on board, but only for selected flights, typically dependent on the origin of the flight. Additionally, most countries reserve the right to disinsection when there is a perceived threat of vector borne disease, for protection of public health, agriculture and the environment.

Pyrethroids are the class of pesticide chemicals currently recommended by the World Health Organization (WHO) for aircraft cabin disinsection (WHO, 1998; Rayman, 2006). The WHO recommends four pyrethroids as active disinsection ingredients: resmethrin, bioresmethrin, d-phenothrin and permethrin (cis/trans ratio of 25/75) (WHO, 1998; Rayman, 2006; Maddalena and McKone, 2008; Mohan and Weisel, 2010). New Zealand and Australia have more recently published guidelines for disinsection of aircraft and approved only the use of d-phenothrin and permethrin (AQIS/MAFBNZ, 2009).

Commonly used pesticide spraying methods for aircraft disinsection can be categorized into five distinct types (Rayman, 2006; Mohan and Weisel, 2010). Three of these methods involve spraying while passengers are on board: “blocks away”, “top of descent” and “on arrival” methods. The two methods that involve spraying in unoccupied cabins are “residual” and “pre-embarkation” methods. Residual application needs to be effective for at least 8 weeks with initial surface loadings of $50 \mu\text{g cm}^{-2}$ and $20 \mu\text{g cm}^{-2}$ of active ingredient on rugs and other cabin surfaces, respectively (Rayman, 2006; AQIS/MAFBNZ, 2009). To achieve this the floor is sprayed twice. The air conditioning system is turned off while the recirculation fans may be left on if essential to the operation of the aircraft. The WHO recommended level for other spraying applications is 7 mg of active ingredient per m^3 of cabin volume (WHO, 1998). Pre-embarkation cabin treatment is also conducted prior to the commencement of passengers boarding but is expected to last only for the duration of a single flight. During disinsection and for a period of 5 min after the completion of the spray, the aircraft’s air conditioning system is switched off.

During the “top of descent” cabin treatment, pesticide is sprayed in an occupied cabin immediately prior to the aircraft commencing its descent to the airport of arrival (AQIS/MAFBNZ, 2009). The air conditioning system operates at normal flow conditions and the recirculation fans remain on during the treatment. During “on arrival” disinsection and for a period of 5 min after completion of the spray, the aircraft’s air-conditioning remains off. The air conditioning system is resumed after 5 min. However the passengers remain seated until clearance is given allowing passengers to disembark. In “blocks away” disinsection the insecticide spray is applied just before the aircraft begins taxiing for takeoff (Gratz et al., 2000). In all the cases, the deposition of pesticide on surfaces is the primary defense against

target insects, because it kills the target insects on contact, and remains active for extended period of time.

Exposures of flight crew and passengers to pesticides sprayed in aircraft cabins can occur via inhalation, dermal contact, or indirect ingestion. Exposure levels can be highly dependent upon the pesticide spraying method employed and upon the time since last application. Even though application of pyrethroid pesticides for aircraft disinsection has been reviewed and approved by the WHO (WHO, 1998; Rayman, 2006), concerns have been raised in the recent past about their potential adverse health effects (Van Netten, 2002; Murawski, 2005), and anecdotal cases of adverse health effects attributed to aircraft disinsection have been reported (Murawski, 2005; Sutton et al., 2007). Sutton et al. (2007) noted that better education of the cabin crew and taking steps to reduce exposures remain the main options until non-toxic alternatives are adopted or sanctioned by countries that require disinsection. Recent toxicological studies have also identified adverse neurological effects of pyrethroids via interaction with sodium channels in the axons of peripheral and central nervous systems in rats (Soderlund, 2012). Early life exposures to pyrethroids can affect the onset of age-related diseases in rats (Carloni et al., 2012), and prenatal exposures to pyrethroids influence vascular development of fetal brain in mice (Imanishi et al., 2012). The question of long term risks versus benefits of pyrethroid application in aircraft cabins has been gaining attention only recently.

There are limited measurement studies reported on pesticide levels measured in aircraft cabins. Berger-Preiss et al. (2004, 2006) conducted experiments in unoccupied aircraft cabins at ground level to study exposures resulting from in-flight spraying of pesticides for the “pre-embarkation” and “top of descent” methods. While they reported low levels of potential inhalation and dermal exposures, there was significant variability in the measurements, and the spatial variability of air and surface concentrations were not characterized. Additionally, the presence of passengers in the “top of descent” case can significantly affect the flow field and concentration profiles (Singh et al., 2002; Mazumdar et al., 2011).

Mathematical and computer simulation models for studying pesticide concentration include the work of Sutton et al. (2007), who modeled the pesticide as aerosol particles and accounted for the differential gravitational settling rates of particles with different aerodynamic diameters. Maddalena and McKone (2008) modeled the pesticide as an inert chemical species and simulated the deposition of pesticide by using parametrizations for surface thickness, deposition rate coefficients, and deposition velocity. However, one limitation of both these models is that assume uniform mixing of pesticide throughout the cabin volume, and therefore cannot characterize the substantial variability of deposition profiles with each type of cabin surface reported by Berger-Preiss et al. (2004, 2006).

Computational Fluid Dynamics (CFD) models provide a means to study concentration and deposition profiles at high spatial and temporal resolutions in aircraft cabin environments (Poussou et al., 2010; Rai and Chen, 2012; Liu et al., 2012). The CFD model in this study was developed based on previously evaluated approximations for flow modeling and contaminant transport in aircraft cabins (Mazumdar and Chen, 2008; Mazumdar et al., 2011;

Poussou et al., 2010), with specific focus on spatial variability of pesticide concentrations and depositions across the cabin when passengers are directly exposed to the sprayed pesticide. The model was evaluated using data from controlled experiments conducted in a cabin mockup facility.

2. Approach

2.1. Experiments in aircraft cabin mockup

The cabin mockup used in this study was a 32 feet long, 11-row, 77 seat twin aisle mockup, located at a Kansas State University facility in Manhattan, KS. All seats were occupied by thermal manikins in order to simulate the temperature difference between a person's body surface and surrounding air in the cabin. Fig. 1 shows the internal structure of the mockup in relation to a full aircraft cabin, measurement locations of manikins, and the aisles along which personnel walk through for spraying the pesticides. Additional details of the mockup can be found in Jones (2009). Two overhead linear inlets at the center of the cabin supplied air to the cabin, and there was no recirculation of air.

Two persons simulated the application of pesticide by crew members, as shown in Fig. 1(b). They walked simultaneously along the aisle from Row 1 toward Row 11 spraying the pesticide sideways in one case and overhead in the other. After spraying, the crew members walked out of the cabin through exit doors located at the end of the aisle behind Row 11. Each person held two canisters of disinsectant. Two most commonly used commercial aircraft disinsection products, one containing 2% d-phenothrin and the second containing 2% permethrin by weight, were sprayed. The cabin setup was similar to the "top of descent" disinsection method with passengers on board.

Pesticide depositions were measured near the passengers at seats 3D at Row 3; 6A, 6D, 6G at Row 6 and 9D at Row 9 (Fig. 1(c)) for a high ventilation scenario and a low ventilation scenario. The high ventilation case was assumed to represent a "top-of-descent" spraying, while the low ventilation rate case was assumed to represent an approximation of "blocks-away" spraying, as well an approximation of worst-case inhalation exposure scenario for spraying with passengers on board. The middle row seats (6A, 6D, and 6G) were selected for evaluation in order to minimize the artificial wall effects in the mockup's truncated structure; such effects would not be present in an actual aircraft. Seats were also selected to capture concentration profiles at locations closer to windows on both sides (6A and 6G); at locations in the middle (3D, 6D, and 9D); and toward the front (3D) and rear of the aircraft (9D) to evaluate the distribution of the deposition profiles across the entire aircraft.

Deposition samples were collected using 9 cm Whatman circle filters placed in opened petri dishes. They were left open from start of spraying up to a period of 20–30 min (lower time for high ventilation scenarios), to ensure that the deposition is completed and only minimal amounts of the pesticide were in the cabin mockup air. The petri dishes were then sealed with a cap and stored at $-10\text{ }^{\circ}\text{C}$ until extracted in 30 mL HPLC grade hexanes containing an internal standard ($500\text{ ng }\mu\text{L}^{-1}$ 1-chloronaphthalene) by ultrasonication for 45 min, followed by mechanical shaking for 5 min. The eluants were centrifuged and the clear supernate was

concentrated to 0.2 mL. Analysis for chemical analysis by extraction followed by gas chromatography/mass spectrometry (HP 6890GC/5973MSD).

2.2. CFD modeling

The CFD model of the 11 row twin-aisle airliner cabin mockup is shown in Fig. 1(c), and was designed based on the geometry of the mockup using a total of 4.5 million tetrahedral cells. Ventilation was modeled via two overhead linear inlets at the center of the cabin and via two linear outlets located near the side walls at floor level. The cabin model is based on the approach used by Mazumdar and Chen (2008), customized for the geometry of the cabin mockup. For all 77 passengers, surfaces such as the lap of the passengers, passengers (whole body), top of seats and back of seats were represented as separate surfaces so that the concentrations for each type of surface can be directly extracted without requiring interpolation in post processing. Similarly, the model also included a $0.1 \text{ m} \times 0.1 \text{ m} \times 0.1 \text{ m}$ cubical volume located at the breathing level (1 m above the floor) of each passenger.

The model was built using the CFD program FLUENT with flow formulations that were previously evaluated with experimental data (Zhang et al., 2009). Re-Normalization Group (RNG) κ - ε model was used to model the turbulence inside the cabin as it had been successful in modeling diverse indoor airflows (Zhang et al., 2007). Furthermore, at low ventilation rates, the airflow inside the cabin is predominately due to thermal buoyancy created by temperature differential between body surface and cabin air, and RNG κ - ε turbulence model has been effective in predicting such flows (Gan, 1998). Simulations were done for two different air exchange rates: 29 ACH and 1 ACH. The 29 ACH case ($1400 \text{ cubic feet min}^{-1}$) corresponds to the typical operating flow rate of the mockup, while the 1 ACH case ($48 \text{ cubic feet min}^{-1}$) was an approximation of the mockup operation with forced ventilation turned off. The thermal boundary conditions during the experiments were also not measured and hence the CFD model used the boundary conditions presented in Table 1 which are similar to that used by Mazumdar and Chen (2008). In short, a temperature boundary condition was used for all surfaces, which limits unrealistic rise in temperature under low ventilation rates.

The 1 ACH scenario approximation used forced ventilation in the case of the CFD simulation, while the cabin mockup had natural ventilation that was not measured. It is not feasible to capture the flow due to natural ventilation at low ventilation rates, so the inlet flow assumption was used as an approximation because of the following reasons: (a) at low air exchange rates the airflow within a cabin is thermal plume dominated and the effect of inlet airflow on the airflow patterns is low, (b) the rise in temperatures under these conditions is limited due to the use of thermal boundary conditions, and (c) at low air exchange rates, pesticide in the air is removed primarily due to deposition on surfaces. In order to evaluate the impact of different flow rates on deposition characteristics, flow simulations were performed at 0.5 ACH, 1 ACH, and 2 ACH using a single row cabin model with periodic boundary conditions at ends. The flow structures across the cabin cross-section for these cases were similar (results not shown), and were primarily governed by thermal plumes. Additionally, a screening level estimation, using the approach of Sutton et al.

(2007), indicated that the impact of low air exchange rates on deposition was less than 2% across air exchanges between 0 and 1.

The CFD model assumed that 776.5 mg of pesticide was sprayed inside the cabin for each scenario, and that the sideways and overhead spraying were done at heights of 1.5 m and 1.8 m above the floor respectively in all the cases, as shown in Fig. 1(d). The spraying amount was based on an estimation of 8 s time for spraying, and estimated via separate experiments where the cans were sprayed for 8 s and the difference in the mass of the cans was measured. A mean value of 776.5 mg for 8 s spraying was obtained from repeated sprayings. The cabin surface area to volume ratio from the CFD model was $3.78 \text{ m}^2 \text{ m}^{-3}$. To simulate a moving spray, the pesticide release was modeled using a series of 8 sequential linear sources along the length of the cabin. Each source remained active for a second, as the sources became sequentially active from Row 1 toward Row 11.

2.3. CFD solution scheme

The pesticide was modeled as an inert species, and the transport of the pesticide was assumed to follow the flow patterns and gravitational deposition. The airflow was assumed not to be affected by the spraying of the pesticide, thus allowing separate solution of a steady state airflow, and an unsteady state contaminant transport.

Concentration and deposition profiles were solved using the transport equation:

$$\frac{\partial(\rho VC)}{\partial t} + \nabla \cdot (\rho A \vec{v} C) = -\nabla \cdot J - R_d + S \quad (1)$$

where, for each tetrahedral cell of volume V considered in the model, \vec{v} is the velocity of airflow in the cell, A is the area normal to the flow, R_d is the net rate of deposition of pesticide from the cell, S is pesticide sprayed into the cell, ρ is the density of air parcel in the cell, and C is the concentration of the contaminant/pesticide.

Additionally, $\nabla \cdot J$ is the rate of mass diffusion of pesticide coefficient, computed using

$$J = -\nabla \cdot \left(\rho D + \frac{\mu_t}{Sc_t} \right) A \nabla C \quad (2)$$

where D is the binary diffusion coefficient of the contaminant/pesticide in air, μ_t is the turbulent viscosity and Sc_t is the turbulent Schmidt number.

Modeling the pesticide as species gave the flexibility to appropriately scale the exposures for any specified amount of pesticide spraying. According to the measurements by Berger-Preiss et al. (2006), aircraft disinsection spray particles have diameters less than $100 \mu\text{m}$. The Stokes number (St) for $100 \mu\text{m}$ particles would be of the order of 10^{-1} assuming a fluid characteristic velocity scale of 0.2 m s^{-1} and a characteristic length scale of 0.05 m (the grid size). For $St \ll 1$, the aerosol particles would follow fluid flow closely.

In general, the drift-flux model has been used by various researchers to simulate aerosol particle dispersion in indoor environments (Murakami et al., 1992; Liu and Zhai, 2007; Zhao

et al., 2004, 2009). The drift flux model addresses the issue of transport of aerosol particles due to the velocity difference between the particles and the air due to slippage. Most studies concluded that fine particles dispersed in a manner similar to species without any slippage because of the small settling velocities (Zhao et al., 2009). Murakami et al. (1992) concluded that aerosol particles smaller than 4.5 μm can be modeled as a passive specie. Liu and Zhai (2007) found that the slippage in sub-20 μm particles can be neglected (Liu and Zhai, 2007; Zhao et al., 2009). Recent investigations (Gupta et al., 2011) show that the aerosol particles exhaled out from a cough followed the bulk airflow in the cabin after an initial transience of 0.5 s. It is also concluded that the volatile matter in aerosol droplets is evaporated as fast as 0.005 s for 0.4 μm and 0.3 s for 30 μm aerosols under in-flight conditions. Thus the volatile matter in the pesticide aerosols would evaporate within a second leaving behind a much finer non-volatile matter. The particle sizes of the pesticide aerosols were not measured during the experiments. Our investigations models the pesticide as species which follows the bulk airflow in the cabin.

The deposition of pesticide on the cabin surfaces was modeled using the species reaction module in FLUENT. In this formulation, the reactant at the cabin surfaces is the pesticide in gaseous phase in the cell adjacent to the surface, and is assumed to be converted to a product that is absorbed on to the surface. Since the chemical characteristics are not changed, the stoichiometric coefficient of this reaction is 1. The deposition characteristics were also assumed to be identical across all cabin surfaces. A portion of the pesticide within the volume of a tetrahedral cell is assumed be deposited on to a surface in direct contact with the cell governed by a reaction rate determined by the Arrhenius kinetic expression:

$$k_d = BT^\beta \exp(-E_a/RT) \quad (3)$$

where B is the pre-exponential factor, T is the temperature, β is the temperature exponent, E_a is the activation energy of the deposition process and R is the universal gas constant (Fluent, 2009). Under a constant temperature, the rate constant k_d is constant throughout the cabin volume. In order to simplify the formulation, the constants β and E_a for the deposition process were set to 0, and so k_d is governed by an effective rate constant B^* . Volatilization and re-suspension of pesticide were assumed to be negligible within the time period of simulation (of the order of 20 min). The influence of movement of cabin crew was not modeled, even though it has an impact on concentration levels at low time scales (Mazumdar et al., 2011). Additionally, the cabin mockup was assumed to be symmetric and impact of imperfections in the interior surfaces of the cabin mockup was assumed to be negligible. These approximations result in deposition dynamics that are stable under different grid sizes (Wang et al., 2012).

At very high values of B^* , all the pesticide within a cell is deposited on to a cabin surface in direct contact with the cell. Very low values of B^* correspond to scenarios where the deposition is negligible. Sensitivity simulations performed for different values of $B^* \in 10^{-6}$, 10^{-3} , 1, 10^3 , 10^6 indicated that the net deposition profiles did not change significantly between 10^3 and 10^6 , and were substantially lower for $B^* = 1$. The pre-exponential factor of 10^3 was used in this study to represent “full absorption” on all surfaces.

Time steps of 0.05 s were used during the first 10 s, and subsequently, time steps of 0.1 s were used. Within each time step, the computations were assumed to be converged when the residual for mass (sum of the absolute residuals in each cell/the total mass inflow) and the residual for energy (sum of the absolute residuals in each cell/the total heat gains) was less than 0.1% and 1% respectively, and when the cumulative normalized residual on the transport equation dropped below 0.001%. Locations of interest (lap, seat top, and breathing volumes) were pre-defined as separate zones, so that the statistics for those locations were computed directly within FLUENT. Cumulative deposition at each location was estimated using the trapezoidal rule for integrating time varying deposition rates.

3. Results

Fig. 2 shows the patterns of airflow across the cabin cross-section for the two air exchanges considered. A cross-section view in the middle of the cabin (Row 6) is shown at 1400 cfm (29 ACH) and 48 cfm (1 ACH). At 29 ACH the inlet air with high momentum is distributed to the side walls, and subsequently flows upwards at the center of the cabin. Furthermore, a nearly symmetric vortex structure is observed across the cabin cross-section. At 1 ACH the thermal plume from the passengers dictates the flow pattern in the cabin. For the cross-section shown, the air rises along the side walls toward the center of the cabin. The flow pattern shown for the 1 ACH case is governed by thermal buoyancy and is in a reverse direction compared to 29 ACH case. The average airflow velocity across the cabin cross-section for the 1 ACH case is about 1/5th of that of the 29 ACH case.

For the high ventilation case (29 ACH) and sideways spraying, Fig. 3 shows the progression of pesticide concentration profiles at the breathing level and of net deposition of pesticide on passengers and seats. Pesticide concentrations fell from above $5000 \mu\text{g m}^{-3}$ at 60 s to below $10 \mu\text{g m}^{-3}$ at 480 s. In the initial few seconds, the breathing zone concentrations are higher near the aisle, while the concentrations were generally lower at the middle seat (e.g. seat D). An asymmetry of pesticide concentration across the cabin cross-section has also been observed. This asymmetry is often attributed to the inherent instability in the combined vortex structure across the cabin cross-section that manifests in modeling results even if the boundary conditions are assumed to be perfectly symmetric (Lin et al., 2005; Poussou et al., 2010). Net deposition was higher on passengers and seats near the aisle, with some seats and passengers experiencing depositions higher than $0.25 \mu\text{g cm}^{-2}$. Note that it is the amount of pesticide deposition expected assuming 100% of the active ingredient settles uniformly on all the surfaces and no pesticide is evacuated out through the cabin ventilation system. The first and last rows (Rows 1 & 11) had lower depositions compared to the other rows. This can be attributed to wall effects and also the fact that the attendants applied the pesticide from the center of the 1st row and stopped at the center of the 11th row. The net deposition on the surface reached a steady level within 240 s, with negligible amount remaining in the cabin air.

For the low ventilation case (1 ACH) and sideways spraying, Fig. 4 shows the corresponding progression of concentrations and surface depositions. In this case, the air concentration levels stayed above $10 \mu\text{g m}^{-3}$ for 1200 s, compared to 480 s in the high ventilation case. The spatial profiles were substantially different from those in the 29 ACH

case. Specifically, the breathing zone concentrations were higher at middle seats (e.g. Seat D), while the air concentrations were generally lower near the window passenger (e.g. Seat A). Likewise, substantially more pesticide was estimated for the middle seats, compared to the sides. In this low ACH case, the deposition at most of the middle row seats was higher than $0.5 \mu\text{g cm}^{-2}$. The net deposition reached close to a steady value at about 1200 s.

For each ventilation scenario, results for sideways and overhead spraying were similar, as shown in Fig. 5. The progression of these concentrations shown in Figs. 3 and 4 indicates that the impact of the spraying patterns on concentration profiles was significant only during a small period of time following the spraying.

The CFD model was evaluated using pesticide deposition data collected from the experiments for the five seats (3D, 6A, 6D, 6G and 9D, as shown in Fig. 1(c)). Comparison of model estimates with measurements for the high ventilation rate is shown in Fig. 6. In each plot, multiple measurement data points for a seat within a specific spray scenario correspond to duplicate measurements within an experiment, repeats of experiments, and experiments conducted with different type of pesticide. Corresponding CFD model results are shown as a box plot for each scenario–location combination. The CFD results reflect estimates for a specific amount of mass of active agent sprayed, thus the corresponding results for permethrin and phenothrin can be estimated from one CFD simulation independent of the chemical sprayed. This assumption is valid in this case because the molecular weights of phenothrin (350.46) and permethrin (391.30) are approximately similar and their physical characteristics are also similar. The CFD model calculates deposition estimates for several small areas that comprise the area of the seat top or lap. For example, the lap area for passengers in seats 3D, 6A, 6D, 6G and 9D had 47, 52, 53, 52 & 46 computational cells, respectively, on the surface. Similarly, the corresponding seat tops had 29, 29, 31, 29 & 29 cells, respectively, on the surface. Therefore, the distribution of CFD estimates for a given location is shown as a box plots showing the mean, minimum, and maximum, as well as the 25th and the 75th percentiles.

The CFD model was able to capture the deposition profiles of pesticides on the lap and seat-top at high air exchange rate. Corresponding comparisons are shown for the low ventilation case in Fig. 7. The CFD results indicate that significant spatial variations are possible under low air exchange rates. In the CFD simulations, the window seats (6A & 6G) showed a substantially lower net deposition compared to the middle seats (3D, 6D & 9D). However, this variation is not nearly as pronounced in the experimental data where the rates are much more uniform. The difference between the experimental and CFD results for the window seats can be attributed to an increased mixing occurring due to the movement of the persons spraying the pesticide and due to imperfections and sharp surfaces in the cabin interior; these effects were not captured by the relatively smooth flow characteristics in the CFD model. In addition, it is difficult to capture low flow rate profiles under natural ventilation conditions because the corresponding inlets and outlets are not well defined. The CFD model estimates as well as the experimental measurements indicate no significant variation in deposition characteristics for sideways and overhead spraying under the high and low air exchange rates.

Surface deposition levels varied from 0.33 to 1.22 $\mu\text{g cm}^{-2}$ for the low-ventilation case compared to 0.05–0.20 $\mu\text{g cm}^{-2}$ for the high ventilation case. The CFD estimates showed a sharper spatial variation, while the measurements indicated a more uniform deposition. This can potentially be attributed to an increased mixing occurring due to the movement of the persons spraying the pesticide and due to imperfections and sharp surfaces in the cabin interior; these effects were not captured by the relatively smooth flow characteristics in the CFD model.

4. Discussion

Evaluation of potential health risks from pesticides sprayed in aircraft cabins has become an important issue in light of new toxicological evidence of adverse neurological and development effects at low levels of several pyrethroids (Das et al., 2008; Breckenridge et al., 2009; DeMicco et al., 2010). However, estimation of potential exposures of cabin crew and passengers has been limited by the amount of experimental and field sampling data available (Mohan and Weisel, 2010). While computational modeling of pesticide deposition is available (Sutton et al., 2007; Maddalena and McKone, 2008), they currently do not characterize the spatial variability within a cabin as well as the impact of thermal plumes caused by the presence of passengers.

CFD models provide a feasible means to study concentration and deposition profiles at high spatial and temporal resolutions in aircraft cabin environments, and can account for the effects of thermal plumes (Poussou et al., 2010; Rai and Chen, 2012; Liu et al., 2012). However, substantial resources are required for developing the cabin interior geometry and to define a mesh with adequate resolution that can capture the major components of interest. In the current study, the transport processes were assumed to be independent of the bulk airflow processes, so the same airflow calculations can be used for different spray and deposition assumptions for a given air exchange rate. In fact, multiple release patterns and deposition rate coefficients were incorporated into the model as a set of different independent chemical species, each of which was tracked separately within a single simulation.

The CFD model simulated the measured depositions of pesticide across the cabin reasonably well for the high air-exchange rate. The differences observed at lower air exchange rates can be attributed to increased mixing within the cabin due to the movement of persons spraying the pesticide and due to imperfections, which warrant further investigation. Additionally, since the low ventilation experiments were conducted under a natural flow (i.e. no forced ventilation), the exact air exchanges were not measured when the experiments were performed, and the ventilation characteristics were approximated using a ventilation rate of 1 ACH through the inlets and outlets used for forced ventilation. Additional sources of uncertainties and errors arise from simplifying assumptions: (a) the spraying rate was uniform within and across each experiment, and (b) all releases within each spraying type scenario occurred at the same height.

Overall, the CFD modeling presented here is able to provide high resolution spatial and temporal maps of air concentrations and surface depositions. These estimates can be scaled

for different rates of sprays provided the spraying rate remains uniform for the duration of the spray. Additionally, the ranges of estimates provided by the CFD model, both for different locations as well as for small areas within a given seat, can provide a range of potential exposure conditions that a cabin crew member or a passenger is likely to be exposed to.

5. Conclusion

A new CFD model was developed for studying pesticide concentrations and depositions following spraying within a portion of an aircraft cabin. This model was evaluated with data from spraying experiments conducted in a cabin mockup. The model was able to capture the deposition characteristics and showed substantial variations in deposition profiles that were primarily driven by differences in ventilation rates. The approach employed in this study with respect to species deposition and transport is directly applicable to other types of cabin geometries. Overall, the surface deposition of pesticides was found to be under $0.5 \mu\text{g cm}^{-2}$ for the 25 ACH case and under $1.0 \mu\text{g cm}^{-2}$ for the 1 ACH case, with some areas along the aisle and center experiencing higher concentrations than other areas. These numbers are about 1/40th to 1/20th of the guidance level for residual application (which is expected to be effective for a period of about 56 days). The spatial variation in the deposition characteristics across different cabin surfaces should be investigated in the context of highly exposed individuals.

Acknowledgments

This study was supported primarily by the U.S. Federal Aviation Administration (FAA) Office of Aerospace Medicine through the Air Transportation Center of Excellence for Airliner Cabin Environment Research (ACER), Cooperative Agreement 04-C-ACE-UMDNJ. Additional support was provided by the NIEHS sponsored UMDNJ Center for Environmental Exposures and Disease, Grant NIEHS P30ES005022. The views expressed in this manuscript are solely of the authors and do not necessarily reflect those of the funding agencies. The funding agencies neither endorse nor reject the findings of this study. The authors gratefully acknowledge Dr. Qianyan Chen for comments and input into the manuscript.

References

- AQIS/MAFBNZ. Schedule of Aircraft Disinsection Procedures, Version 2.0. Australian Quarantine and Inspection Service and Ministry of Agriculture and Forestry Biosecurity; New Zealand: 2009.
- Berger-Preiss E, Koch W, Behnke W, Gerling S, Kock H, Elflein L, Appel K. In-flight spraying in aircrafts: determination of the exposure scenario. *International Journal of Hygiene and Environmental Health*. 2004; 207:419–430. [PubMed: 15575556]
- Berger-Preiss E, Koch W, Gerling S, Kock H, Klasen J, Hoffmann G, Appel K. Aircraft disinsection: exposure assessment and evaluation of a new pre-embarkation method. *International Journal of Hygiene and Environmental Health*. 2006; 209:41–56. [PubMed: 16373201]
- Breckenridge C, Holden L, Sturgess N, Weiner M, Sheets L, Sargent D, Soderlund D, Choi J, Symington S, Clark J, Burr S, Ray D. Evidence for a separate mechanism of toxicity for the Type I and the Type II pyrethroid insecticides. *Neurotoxicology Suppl*. 2009; 1:S17–S31.
- Carloni M, Nasuti C, Fedeli D, Montani M, Amici A, Vadhana MD, Gabbianelli R. The impact of early life permethrin exposure on development of neurodegeneration in adulthood. *Experimental Gerontology*. 2012; 47 (1):60–66. [PubMed: 22056222]
- Das P, Streit T, Cao Y, Rose R, Cherrington N, Ross M, Wallace A, Hodgson E. Pyrethroids: cytotoxicity and induction of CYP isoforms in human hepatocytes. *Drug Metabolism and Drug Interactions*. 2008; 23 (3–4):211–236. [PubMed: 19326768]

- DeMicco A, Cooper K, Richardson J, White L. Developmental neurotoxicity of pyrethroid insecticides in zebrafish embryos. *Toxicological Sciences*. 2010; 113 (1):177–186. [PubMed: 19861644]
- Fluent. Ansys Fluent 12.0. User's Guide. FLUENT Inc; 2009.
- Gan G. Prediction of turbulent buoyant flow using an RNG κ - ϵ model. *Numerical Heat Transfer, Part A: Applications*. 1998; 33 (2):169–189.
- Gratz NG, Steffen R, Cocksedge W. Why aircraft disinsection? *Bulletin of the World Health Organization*. 2000; 78 (8):995–1004. [PubMed: 10994283]
- Gupta J, Lin CH, Chen Q. Transport of expiratory droplets in an aircraft cabin. *Indoor Air*. 2011; 21 (1):3–11. [PubMed: 21208287]
- Imanishi S, Okura M, Zaha H, Yamamoto T, Akanuma H, Nagano R, Shiraishi H, Fujimaki H, Sone H. Prenatal exposure to permethrin influences vascular development of fetal brain and adult behavior in mice offspring. *Environmental Toxicology*. 2012
- Jones, B. Advanced models for predicting contaminants and infectious disease virus transport in the airliner cabin environment: experimental data. *Proceedings of the Transportation Research Board, Research on the Transmissions of Disease in Airports and Aircraft, A Symposium; The National Academies; Sep. 2009*
- Lin CH, Horstman R, Ahlers M, Sedgwick L, Dunn K, Topmiller J, Bennett J, Wirogo S. Numerical simulation of airflow and airborne pathogen transport in aircraft cabins, Part I: numerical simulation of the flow field. *ASHRAE Transactions*. 2005; 111 (1):755–763.
- Liu X, Zhai Z. Identification of appropriate CFD models for simulating aerosol particle and droplet indoor transport. *Indoor and Built Environment*. 2007; 16:322–330.
- Liu W, Mazumdar S, Zhang Z, Poussou S, Liu J, Lin CH, Chen Q. State-of-the-art methods for studying air distributions in commercial airliner cabins. *Building and Environment*. 2012; 47:5–12.
- Maddalena R, McKone T. Pesticide exposures on commercial aircraft: a literature review and screening level exposure assessment. *Tech rep*. 2008
- Mazumdar S, Chen Q. Influence of cabin conditions on placement and response of contaminant detection sensors in a commercial aircraft. *Journal of Environmental Monitoring*. 2008; 10:71–81. [PubMed: 18175019]
- Mazumdar S, Poussou S, Lin CH, Isukapalli S, Plesniak M, Chen Q. Impact of scaling and body movement on contaminant transport in airliner cabins. *Atmospheric Environment*. 2011; 45:6019–6028.
- Mohan K, Weisel C. Sampling scheme for pyrethroids on multiple surfaces on commercial aircrafts. *Journal of Exposure Science & Environmental Epidemiology*. 2010; 20:320–325. [PubMed: 19756041]
- Murakami S, Kato S, Nagano S, Tanaka Y. Diffusion characteristics of airborne particles with gravitational settling in a convection-dominant indoor flow field. *ASHRAE Transactions*. 1992; 98:82–97.
- Murawski, J. Air Quality in Airplane Cabins and Similar Enclosed Spaces. *The Handbook of Environmental Chemistry*. Vol. 4(H). Springer; Berlin/Heidelberg: 2005. Insecticide use in occupied areas of aircraft; p. 169-190.
- Poussou S, Mazumdar S, Plesniak M, Sojka P, QC. Flow and contaminant transport in an airliner cabin induced by a moving body: scale model experiments and CFD predictions. *Atmospheric Environment*. 2010; 44 (24):2830–2839.
- Rai A, Chen Q. Simulations of ozone distributions in an aircraft cabin using computational fluid dynamics. *Atmospheric Environment*. 2012; 54:348–357.
- Rayman R. Aircraft disinsection. *Aviation, Space and Environmental Medicine*. 2006; 77 (7):733–736.
- Singh A, Hosni M, Horstman R. Numerical simulation of airflow in an aircraft cabin section. *ASHRAE Transactions*. 2002; 108 (1):1005–1013.
- Soderlund D. Molecular mechanisms of pyrethroid insecticide neurotoxicity: recent advances. *Archives of Toxicology*. 2012; 86:165–181. [PubMed: 21710279]
- Sutton P, Vergara X, Beckman J, Nicas M, Das R. Pesticide illness among flight attendants due to aircraft disinsection. *American Journal of Industrial Medicine*. 2007; 50:345–356. [PubMed: 17407145]

- USDOT. Aircraft Disinsection Requirements (On-line). US Department of Transportation; Washington, DC: 2010. Available from: <http://ostpxweb.dot.gov/policy/safetyenergyenv/disinsection.htm> [accessed 15.06.12]
- Van Netten C. Analysis and implications of aircraft disinsectants. *Science of the Total Environment*. 2002; 293 (1–3):257–262. [PubMed: 12109478]
- Wang M, Lin CH, Chen Q. Advanced turbulence models for predicting particle transport in enclosed environment. *Building and Environment*. 2012; 47:40–49.
- WHO. Tech rep. 1998. Recommendations on the Disinsecting of Aircraft.
- Zhang Z, Chen X, Mazumdar S, Zhang T, Chen Q. Experimental and numerical investigation of airflow and contaminant transport in an airliner cabin mockup. *Building and Environment*. 2009; 44 (1):85–94.
- Zhang Z, Zhang W, Zhai Z, Chen Q. Evaluation of various turbulence models in predicting airflow and turbulence in enclosed environments by CFD: Part-2: comparison with experimental data from literature. *HVAC&R Research*. 2007; 13 (6):871–886.
- Zhao B, Chen C, Tan Z. Modeling of ultrafine particle dispersion in indoor environments with an improved drift flux model. *Journal of Aerosol Science*. 2009; 40:29–43.
- Zhao B, Li X, Zhang Z. Numerical study of particle deposition in two different kind of ventilated rooms. *Indoor and Built Environment*. 2004; 13:443–451.

HIGHLIGHTS

- Disinsection of aircraft is required by some countries on international flights.
- Computational Fluid Dynamics model for pesticides in aircraft was developed/evaluated.
- CFD model predicted loading at 29 ACH well, but underestimated some levels at 1 ACH.
- CFD model provided high resolution air and loading estimates for pesticide exposures.

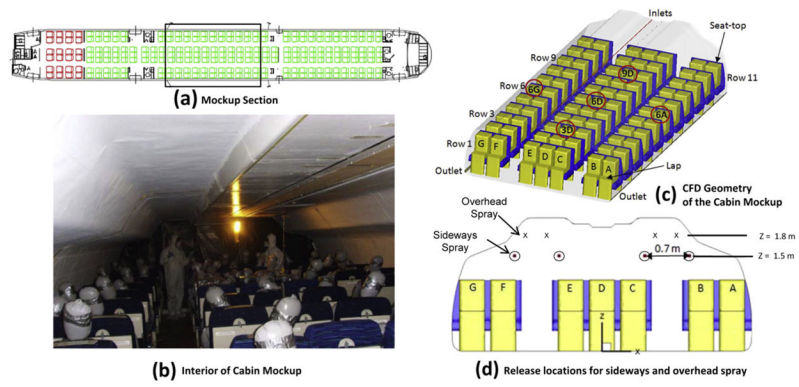


Fig. 1. (a) Layout of a twin-aisle cabin of an aircraft; (b) the 11-row twin-aisle cabin mock-up at Kansas State University; and (c) schematic of the cabin layout in the CFD model along with seats where measurements were made, and (d) cross-sectional view showing release locations.

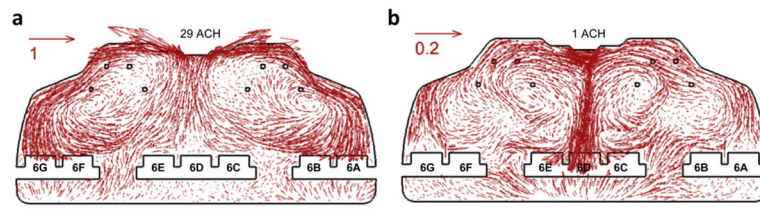


Fig. 2. Comparison of CFD estimates of airflows across the cabin cross-section for (a) 1400 cfm (29 ACH) and (b) 48 cfm (1 ACH).

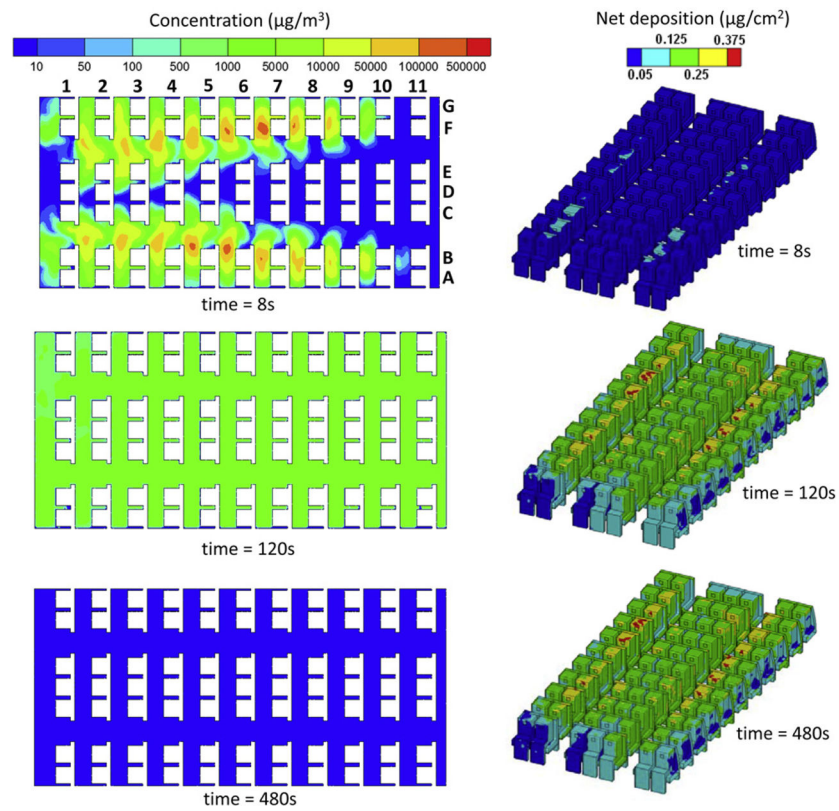


Fig. 3. Progression of breathing level concentrations and net surface deposition following sideways spraying under 1400 cfm (29 ACH) ventilation. Plots for the 29 ACH case and 1 ACH case use different scales.

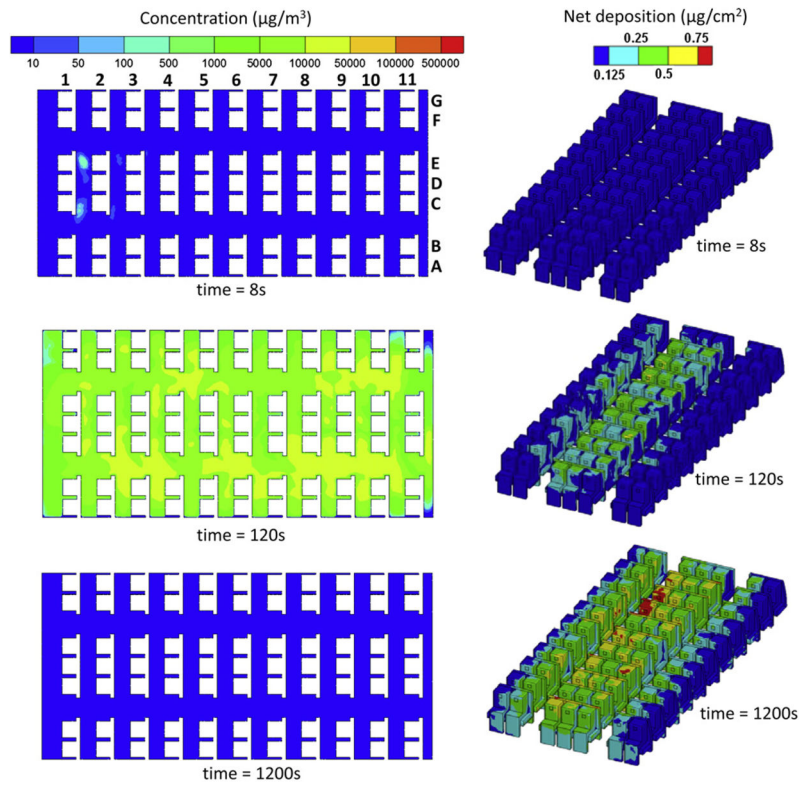


Fig. 4. Progression of breathing level concentrations and net surface deposition following sideways spraying under 48 cfm (1 ACH) ventilation.

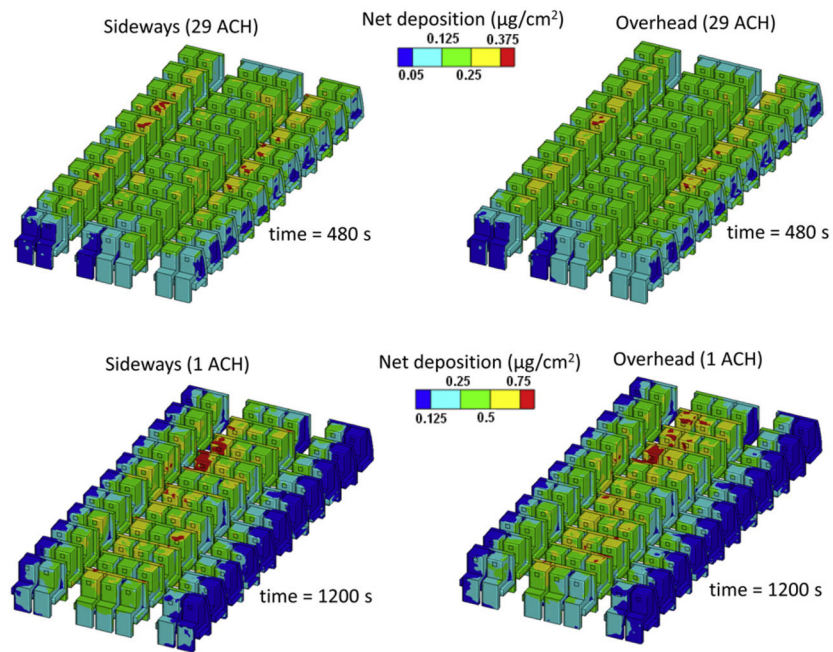


Fig. 5. Profiles of net surface deposition of pesticide for sideways and overhead spraying under the 1 ACH and 29 ACH ventilation scenarios.

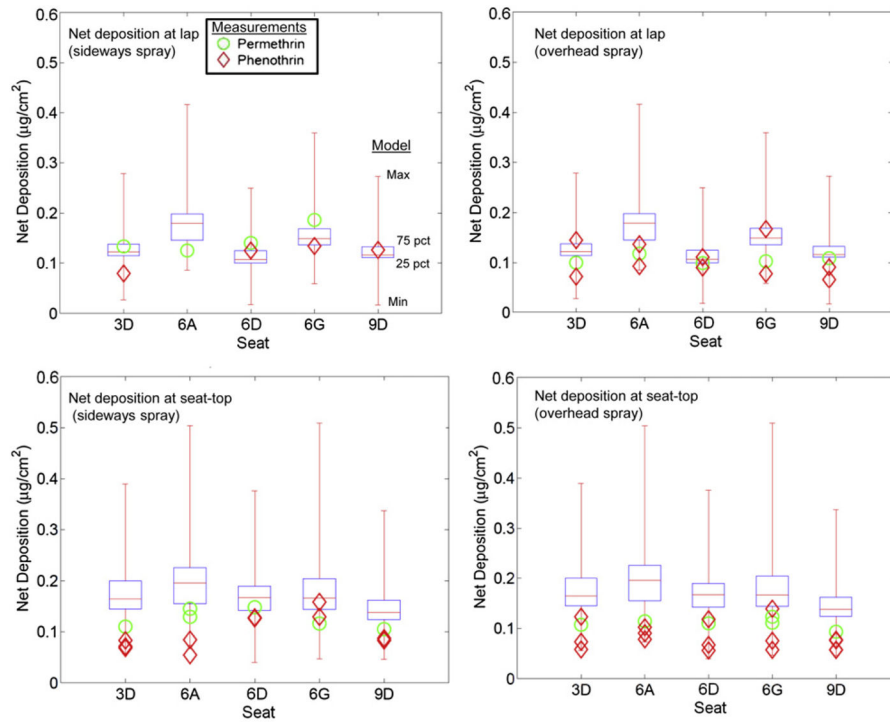


Fig. 6. Comparison of CFD predictions (box plot) with experimental measurements for the high ventilation scenario (29 ACH). The CFD estimates over multiple, small cells at a given seat or lap are shown as a box plot, and the corresponding measurements are shown as points. Multiple measurement data points reflect duplicate measurements in an experiment, repeats of experiments, and experiments conducted with different type of pesticide.

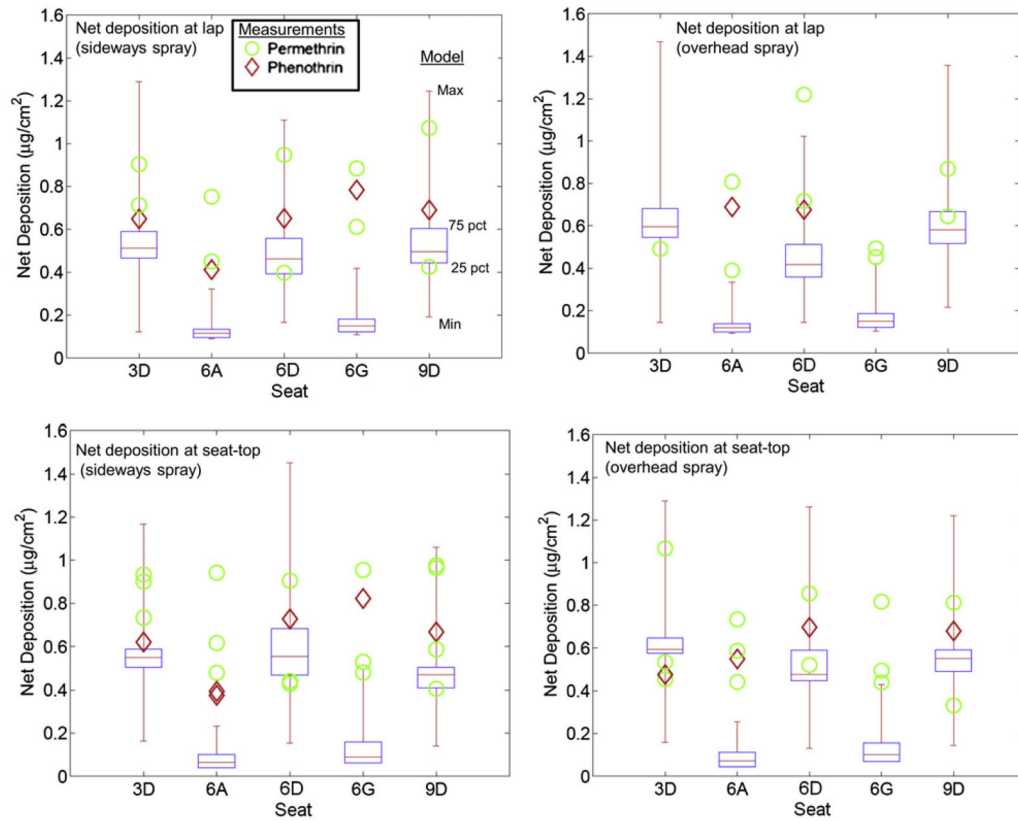


Fig. 7. Comparison of CFD predictions (box plot) with experimental measurements for the low ventilation scenario (1 ACH). The CFD estimates over multiple, small cells at a given seat or lap are shown as a box plot, and the corresponding measurements are shown as points. Multiple measurement data points reflect duplicate measurements in an experiment, repeats of experiments, and experiments conducted with different type of pesticide.

Table 1

Thermal boundary conditions used for the 11-row airliner cabin.

| | |
|--------------------------|-----------|
| Supply air temperature | 19.5 °C |
| Ceiling | 23 °C |
| Side walls | 18 °C |
| Floor under center seats | 24 °C |
| Passengers | 30.3 °C |
| Floor under side seats | 23 °C |
| Seats | Adiabatic |